Talanta 126 (2014) 130–135

Contents lists available at ScienceDirect

Talanta

journal homepage: www.elsevier.com/locate/talanta

An aptamer-based quartz crystal microbalance biosensor for sensitive and selective detection of leukemia cells using silver-enhanced gold nanoparticle label

Wenqian Shan [a], Yuliang Pan [a], Heting Fang [a], Manli Guo [a,b,*], Zhou Nie [a], Yan Huang [a], Shouzhuo Yao [a]

[a] State Key Laboratory of Chemo/Biosensing and Chemometrics, College of Chemistry and Chemical Engineering, Hunan University, Changsha 410082, China
[b] School of Chemistry and Environment, South China Normal University, Guangzhou 510006, China

ARTICLE INFO

Article history:
Received 25 December 2013
Received in revised form
18 March 2014
Accepted 24 March 2014
Available online 29 March 2014

Keywords:
Quartz crystal microbalance (QCM)
Aminophenylboronic acid (APBA)
Gold nanoparticles (AuNPs)
Silver enhancement
Leukemia cell detection

ABSTRACT

An aptamer-based quartz crystal microbalance (QCM) biosensor was developed for the selective and sensitive detection of leukemia cells. In this strategy, aminophenylboronic acid-modified gold nanoparticles (APBA-AuNPs) which could bind to cell membrane were used for the labeling of cells followed by silver enhancement, through which significant signal amplification was achieved. Both the QCM and fluorescence microscopy results manifested the selectivity of the sensor designed. A good linear relationship between the frequency response and cell concentration over the range of 2×10^3–1×10^5 cells/mL was obtained, with a detection limit of 1160 cells/mL. This approach provides a simple, rapid, and economical method for leukemia cell analysis which might have great potential for further use.

1. Introduction

Leukemia, a cancer of the blood or bone marrow, is still one of the most common and aggressive cancers [1]. For the purpose of efficient cure of this disease, sensitive and accurate diagnosis is essential and important. Methods currently used for the detection of leukemia cells include flow cytometry [2], polymerase chain reaction [3], and fluorescence measurement [4]. Nevertheless, many of these methods have associated disadvantages; for example, they are time-consuming, costly and require sophisticated instrumentations. Hence, there is still a need to develop simple and economical methods for selective recognition and sensitive detection of leukemia cells.

Aptamers, obtained by an in vitro process named SELEX (systematic evolution of ligands by exponential enrichment) [5,6], are a kind of artificial single-stranded oligonucleotide strands with special three-dimensional structures. They can selectively recognize and bind to a wide range of targets, such as drugs [7], proteins [8] and even whole cells [9]. In comparison with traditional antibodies, aptamers exhibit several advantages including easy and economical synthesis, ease of purification to a high degree, good stability, and lack of immunogenicity [10]. These unique properties make them useful in the fabrication of various biosensors for leukemia cell detection [11,12]. However, in many of these methods, the aptamers were further conjugated with other materials, such as nanoparticles, which might to some extent decrease the performance of the aptamers. What is more, few efforts have been made in the development of an aptamer-based quartz crystal microbalance (QCM) biosensor for leukemia cell detection. Therefore, the construction of a QCM biosensor using the unmodified aptamer for cancer cell detection is still encouraging.

In recent years, due to the unique optical, chemical and biological attributes, gold nanoparticles (AuNPs) are finding more and more applications in chemical and biological fields, such as metal ions and DNA hybridization detection [13–16], drug delivery [17], cancer diagnostics and therapy [18,19]. Besides, the advantages of AuNPs including facile synthesis, ease of functionalization and good biocompatibility make them suitable to serve as binding agents towards specific targets such as whole cells through appropriate modification. In this article, *p*-aminophenylboronic acid conjugated gold nanoparticles (APBA-AuNPs) were synthesized and used for capturing leukemia cells and then as substrates for silver enhancement, which is an appealing way for signal amplification, owning to a variety of advantages such as simplicity, low cost and high sensitivity. According to a previous report [20], AuNPs could serve as nucleation sites and automatically catalyze the chemical reduction of silver ion into silver metal in the

* Corresponding author at: State Key Laboratory of Chemo/Biosensing and Chemometrics, College of Chemistry and Chemical Engineering, Hunan University, Changsha 410082, China. Tel./fax: +86 731 88821626.
E-mail address: manliguo@163.com (M. Guo).

http://dx.doi.org/10.1016/j.talanta.2014.03.056
0039-9140/

presence of a reducing agent such as hydroquinone (HQ). The QCM technique was applied for detection of the deposited silver metal since it was a device sensitive to the mass change on the electrode surface. It is also worth mentioning that the synthesized particles were very stable when stored at 4 °C.

QCM, a well-known nanogram mass sensing device, has been widely used in biological research fields due to its satisfactory performance, e.g., high sensitivity, rapid and facile operation. Many reports on the design of label-free signal transduction platform for cell-based biosensing have been presented. It has been applied to study the attachment, adhesion and spreading of cells on different substrates [21–23] and response of cells to exogenous stimulations [24–26]. The advantages of QCM in these studies are that it can be used as a continuous monitoring device and can detect cumulative effects in a non-invasive way with high sensitivity. However, there are few reports [27] on the analysis of leukemia cells using QCM.

Herein, an aptamer-based QCM biosensor was fabricated for selective and sensitive determination of acute leukemia cells based on silver-enhanced AuNP label. In this strategy, target leukemia cells were selectively captured by the aptamer immobilized on the QCM sensor surface, then APBA-AuNPs were used to label the cells followed by silver enhancement, and the resonant frequency change of the QCM caused by the deposition of silver metal was monitored in real-time.

2. Experimental

2.1. Materials and apparatus

Aptamer sgc8c, a specific recognition probe for CCRF-CEM cells selected by the cell-SELEX method [28], was used in our work for CCRF-CEM cell detection: sgc8c, 5′-AAA AAA AAA AAT CTA ACT GCT GCG CCG CCG GGA AAA TAC TGT ACG GTT AGA-3′ (Sangon Inc., Shanghai, China). A random nucleotide sequence 5′-TTA GCC ATG CAC CGT GAC ACT CCT GTC AGC ATT CAG AAC C-3′ was used as control. Both sequences were terminated with the 5′-thiol modifier C6 and purified with high-pressure liquid chromatography (HPLC). $HAuCl_4 \cdot 3H_2O$ was purchased from Sigma-Aldrich (St. Louis, USA). *p*-Aminophenylboronic acid ($C_6H_8BNO_2 \cdot H_2O$, APBA) was purchased from Frontier Scientific Services, Inc. (Logan, Utah, USA). 1-Ethyl-3-(3′-(dimethylamino) propyl) carbodiimide (EDC) and N-hydroxysuccinimide (NHS) were purchased from GL Biochem Ltd. (Shanghai, China). APBA-AuNPs were prepared according to our previous report [29]. Ultrapure water (18.2 MΩ cm) from a Millipore Milli-Q system was used throughout.

Chemicals for cell culture were obtained from Gibco (Grand Island, NY, USA). Phosphate-buffered saline (PBS) solution consisting of 136.7 mmol L^{-1} NaCl, 2.7 mmol L^{-1} KCl, 9.7 mmol L^{-1} Na_2HPO_4 and 1.5 mmol L^{-1} KH_2PO_4 was used.

The piezoelectric quartz crystals (AT-cut, 9 MHz, 12.5 mm diameter) with gold electrodes (6.0 mm diameter) on both sides were used. The resonant frequency and resonant resistance of a quartz crystal were measured simultaneously by using a Maxtek Research Quartz Crystal Microbalance (Inficon).

2.2. Cell culture

CCRF-CEM cells (T-cell, human acute lymphoblastic leukemia) were purchased from the Cell Bank of Type Culture Collection of Chinese Academy of Sciences (Shanghai, China), and Romas cells (B-cell, human Burkitt's lymphoma) were purchased from the Cell Bank of Nanjing KeyGen Biotech. Co. Ltd., China. Both types of cells were cultured in RPMI-1640 medium with 10% fetal bovine serum (Gibco) and 100 U mL^{-1} penicillin-streptomycin at 37 °C in water-saturated atmosphere containing 5% CO_2. At the logarithmic phase, the cells were collected by centrifugation at 1000 rpm for 5 min, then washed with PBS, and re-dispersed in sterile PBS for further use. The density of cells was determined using a TC10 automated cell counter (BIO RAD). The fluorescence microscopy images of cells were taken by a Leica DMI4000B microscope (Germany).

2.3. QCM measurements

As reported previously [30], the piezoelectric quartz crystal was sandwiched between two glass tubes with only one side of the crystal wafer exposed to the liquid. The reaction chamber above the crystal wafer was held with a chlorinated polyethylene centrifugal tube (12 mm inner diameter, 1.0 cm length). Similar to previous reports [31,32], before use the gold surface of QCM was pretreated with piranha solution, a 7:3 mixture of concentrated H_2SO_4 and 30% H_2O_2 (caution: such a solution should be handled with extreme care), followed by rinsing thoroughly with ethanol and ultrapure water in sequence and finally drying under a nitrogen flow.

The cleaned QCM Au electrode was exposed to 0.2 mM thiol-terminated aptamer solution for 1 h to obtain the aptamer/Au electrode, followed by rinsing with water to remove the unbound or weakly adsorbed aptamers. Then the electrode was immersed into 1.0 mM 6-mercapto-1-hexanol (MCH) solution for about 30 min to block the uncovered gold surface and make aptamers upright on the electrode. The modified electrode was thoroughly rinsed with ultrapure water. Then 470 μL PBS was added onto the QCM Au electrode, followed by adding 30 μL PBS containing different numbers of cells when the resonant frequency (*f*) became stable. Thirty minutes later, the electrode was washed with PBS and then 100 μL APBA-AuNPs was added into the chamber. After incubation for 30 min, the electrode was rinsed with PBS and ultrapure water, respectively. Freshly prepared silver enhancement solution containing silver nitrate (1.7%) and hydroquinone (3.2%) was added into the chamber and the resonant frequency change was monitored. As a control experiment, the cells were directly treated with silver enhancement solution without treatment of APBA-AuNPs. After each measurement, the liquid was let out, and then the quartz crystal gold electrode was washed with H_2SO_4/H_2O_2 (v/v, 7:3) and water successively for reuse. All the QCM experiments were performed at 25 °C.

2.4. Fluorescence microscopy observation

The cells captured on the sensor surface were also characterized by fluorescence microscopy. After incubation with cells for 30 min, the modified electrode was washed twice with PBS, treated with 0.01% acridine orange (AO) dissolved in PBS for 3 min. Then the cells were washed with PBS, and the fluorescence microscopy images of cells were taken under blue light irradiation with a Leica DMI 4000B microscope.

3. Results and discussion

3.1. Characterization of the APBA-AuNPs

UV–vis absorbance spectroscopy, transmission electron microscopy (TEM) and Fourier transform infrared spectroscopy (FITR) were used for characterization of the APBA-AuNPs synthesized. The results were shown in the recently published report of our group [29].

3.2. Stepwise construction and characterization of the modified electrode

Scheme 1 shows the schematic representation of this QCM detection method based on the APBA-AuNPs amplified assay combined with silver enhancement. Firstly, thiol-terminated aptamer (sgc8c), specific for CCRF-CEM cells, was immobilized on the QCM Au electrode through Au–S bond. Then via the interaction between the cell membrane protein tyrosine kinase-7 (PTK7) and the aptamer [33], CCRF-CEM cells were effectively captured. According to previous reports, sialic acids are one of the most important molecules of life. They are commonly found at the terminal position of the glycans structures on cell membranes, and can form stable five- or six-membered cyclic borate ester complexes with APBA [34]. Based on this property, the synthesized APBA-AuNPs were used to label the captured cells and subsequently as the catalyst for silver ion reduction in the presence of the reducing agent hydroquinone.

The process of aptamer immobilization and subsequent CCRF-CEM cells binding can be sensitively detected by the QCM with a piezoelectric quartz crystal as its central sensing element. A linear relationship existed between the observed shift in resonant frequency and change in surface mass loading of QCM. That was the so-called Sauerbrey equation [35]. The equation is as follows:

$$\Delta f = -2f_0^2\frac{\Delta m}{A\sqrt{\rho\mu}} = (-2.264\times10^{-6})f_0^2\frac{\Delta m}{A}$$

where Δf (Hz) is the measured frequency shift, f_0 (Hz) is the QCM resonant frequency in the fundamental mode in air, Δm (g) is the electrode mass change, A (cm^2) is the piezoelectrically active area, ρ is the density of the quartz (2.648 g cm^{-3}), and μ is the shear modulus of quartz (2.947×10^{11} g cm^{-1} s^{-2} for AT-cut quartz).

The formation of the aptamer self-assembled monolayer was real-time monitored by QCM. As shown in Fig. 1, the aptamer assembly induced a frequency decrease of 117.7 Hz. The change of frequency to some extent suggested the adsorption of aptamer onto the electrode.

After aptamer immobilization and MCH blocking, the sensor was then used for selective capture of cells, and the results are shown in Fig. 2. When incubated with 10,000 CCRF-CEM cells, a pronounced frequency shift of $-\Delta f$=107.8 Hz was observed within 30 min (curve c). In the control experiment, f also decreased when the random sequence-modified electrode was incubated with CCRF-CEM cells (curve b), which was probably due to the deposition of cells onto the sensor surface driven by the gravity effect. Whereas the $-\Delta f$ value (about 39.1 Hz) was much smaller, which indicated that it was not the gravity effect but the binding of CCRF-CEM cells with the aptamer on the sensor surface dominated the QCM response. Another control experiment was also performed using Romas cells as analyte. As shown in Fig. 2, the incubation of the sensor with Romas cells resulted in a little decrease in the resonant frequency of about 35.9 Hz (curve a), suggesting that the aptamer-based QCM biosensor displayed good selectivity toward CCRF-CEM cells. Besides, the binding could

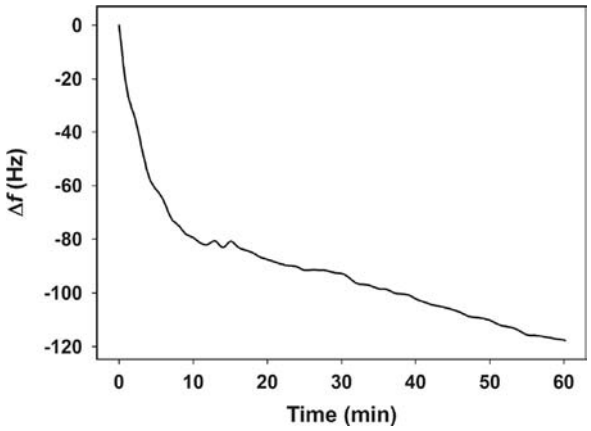

Fig. 1. Real-time frequency response of the QCM to the modification of aptamer.

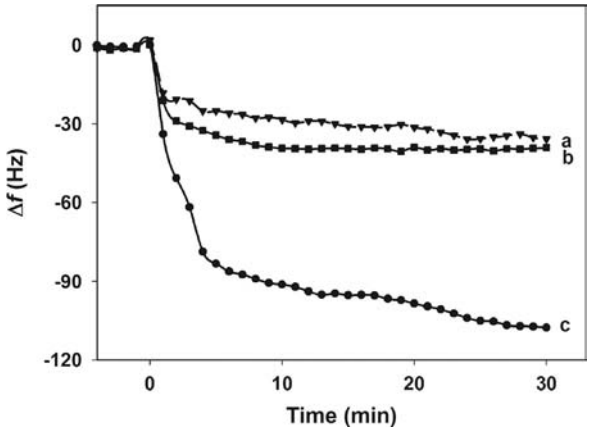

Fig. 2. Resonant frequency responses of different electrodes upon the additions of 10,000 cells: (a) Romas cells added to aptamer-modified surface; (b) CCRF-CEM cells added to random DNA sequence-modified surface; (c) CCRF-CEM cells added to aptamer-modified surface.

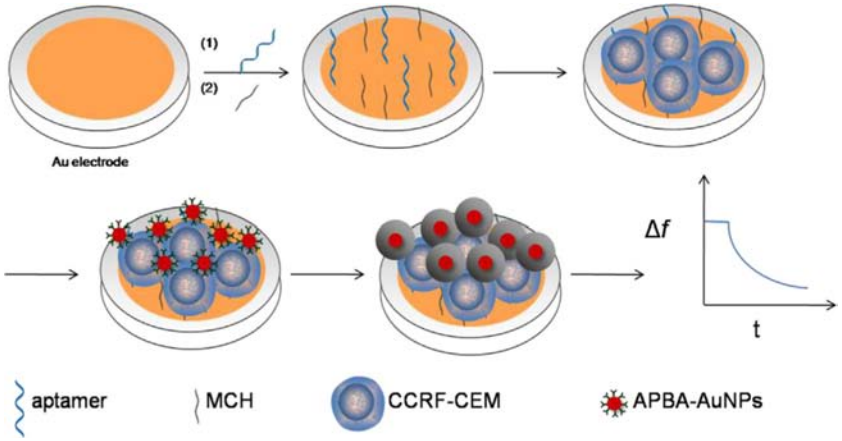

Scheme 1. Schematic representation of the fabrication of the QCM biosensor for analysis of the leukemia cells.

be completed within 30 min, which is a short time for analytical assay.

The capture of CCRF-CEM cells onto the sensor surface was also performed in plasma. In our work, 470 μL plasma was added onto the aptamer-modified QCM Au electrode, followed by adding 30 μL plasma containing 10,000 CCRF-CEM cells when f became stable. A slightly smaller frequency response ($-\Delta f$=93 Hz) was obtained compared with curve c in Fig. 2 (107.8 Hz), suggesting that the detection of cells can be performed in complex biological medium.

Sialic acids existing on cell membranes can form stable borate ester complexes with phenylboronic acid (PBA). Here we use the AuNPs with APBA tags to label the cells captured on the sensor, followed by silver enhancement, with the aim to amplify the frequency response. The immobilization of APBA-AuNPs was monitored with the QCM in real-time (Fig. 3). APBA-AuNPs anchoring to the surface of the cells captured on the QCM Au electrode resulted in a gradual decrease of the frequency ($-\Delta f$=69.7 Hz), indicating the binding of the nanoparticles with the cell surface.

3.3. Detection of leukemia cells using QCM amplified by silver enhancement

With hydroquinone as a reducing agent, AuNPs immobilized on the cell surface could catalyze the chemical reduction of silver ion into metallic silver which subsequently deposited onto the surface of AuNPs. The deposition of metal silver would result in dramatic frequency decrease. In this study, the silver-enhanced AuNP label technique was applied for signal amplification in the QCM detection system. After the incubation of APBA-AuNPs with cells for the required time and subsequent washing steps, silver enhancement solution was added into the detection cell, and a noteworthy frequency drop was observed after a very short time (Fig. 4, curve c). For 10,000 CCRF-CEM cells, the frequency shifts corresponding to cell capture and APBA-AuNPs immobilization were about −107.8 Hz (Fig. 2, curve c) and −69.7 Hz (Fig. 3), respectively. However, after the addition of silver enhancement solution, a much larger frequency response ($-\Delta f$=696.3 Hz) was observed within 10 min, which was a quite increase in output signal. In order to explain the enhanced sensitivity of the strategy, in the control experiments, cells without treatment of APBA-AuNPs were exposed directly to silver enhancement solution, and cells treated with APBA-AuNPs were exposed directly to water. Although the frequency also decreased, the $-\Delta f$ for cells without APBA-AuNPs tags was 6.4 times lower than cells treated with APBA-AuNPs when exposed to silver enhancement solution for 10 min (Fig. 4, curve b). The frequency change induced by water instead of silver enhancement solution (Fig. 4, curve a) could be ascribed to the increase of the liquid level height above the QCM gold electrode. So it can be said that the APBA-AuNPs catalyzed silver enhancement reaction is quite fast, which could help achieve rapid signal amplification and fast analysis of leukemia cells.

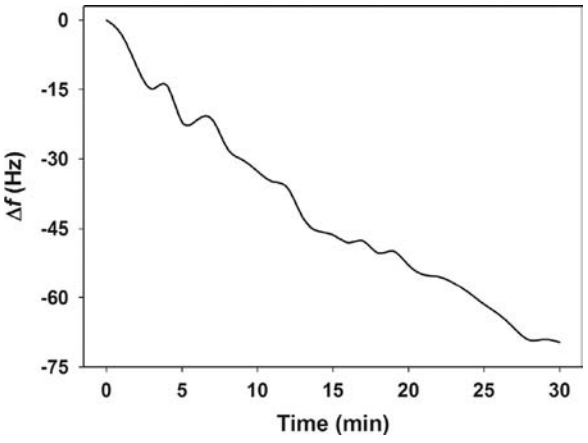

Fig. 3. APBA-AuNPs caused resonant frequency change after binding with the cells captured on the sensor surface for 30 min.

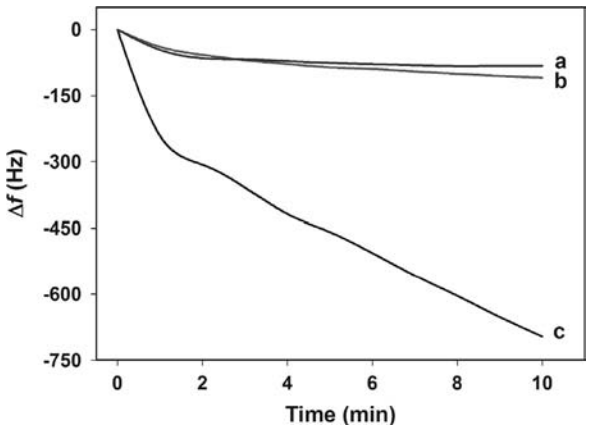

Fig. 4. Frequency responses of the aptamer-based QCM biosensor incubated with cells (2×10^4 cells/mL) when (a) treated with APBA-AuNPs and then exposed to water, (b) directly exposed to silver enhancement solution, and (c) treated with APBA-AuNPs and then exposed to silver enhancement solution.

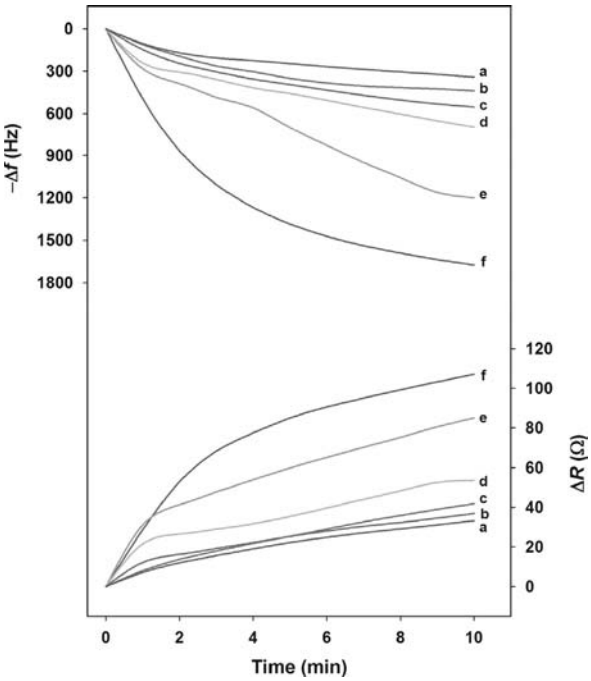

Fig. 5. Resonant frequency and resonant resistance responses during the silver enhancement processes of the aptamer-based QCM sensor incubated with different concentrations of cells followed by APBA-AuNPs labeling. Cell concentrations: (a)–(f) 2×10^3, 6×10^3, 1×10^4, 2×10^4, 6×10^4, and 1×10^5 cells/mL.

Then the quantitative analysis of CCRF-CEM cells was carried out. Fig. 5 shows the resonant frequency and resonant resistance responses during the silver enhancement processes for different concentrations of cells. It can be seen that both $-\Delta f$ and ΔR increased with the increase of CCRF-CEM cell concentration, implying a higher amount of CCRF-CEM cells captured onto the sensor surface. The $-\Delta f/\Delta R$ values were calculated to be 10.3, 11.9, 13.2, 13.0, 14.1, 15.7 Hz Ω^{-1} corresponding to cell concentrations of 2×10^3, 6×10^3, 1×10^4, 2×10^4, 6×10^4, 1×10^5 cells/mL, respectively. All of them were slightly larger than the theoretical value for a net viscodensity effect of an AT-cut 9 MHz crystal, 10 Hz Ω^{-1}, suggesting here that the QCM mass effect dominated the frequency responses [36,37].

A good linear relationship existed between $-\Delta f$ and C_{cells} (cell concentration) over the range from 2×10^3 to 1×10^5 cells/mL (Fig. 6). The regression equation is $-\Delta f = 123.4\ C_{cells} + 397.1$. The detection limit was calculated to be 1160 cells/mL according to the 3σ rule, where σ is the standard deviation of the $-\Delta f$ signal without the addition of CCRF-CEM cells. This was lower than that of 5.0×10^3 cells/mL for HL-60 cells with impedance measurements [38], and also lower than that of 5.75×10^3 cells/mL for acute leukemia using an integrated piezoelectric immunosensor array [39].

The designed biosensor shows attractive performance for the quantification of CCRF-CEM cells, such as a wide linear range and low detection limit. The reason may be as follows: first, aptamer immobilized on the QCM Au electrode provides an ideal interface for cell capture, therefore improving the selectivity of detection.

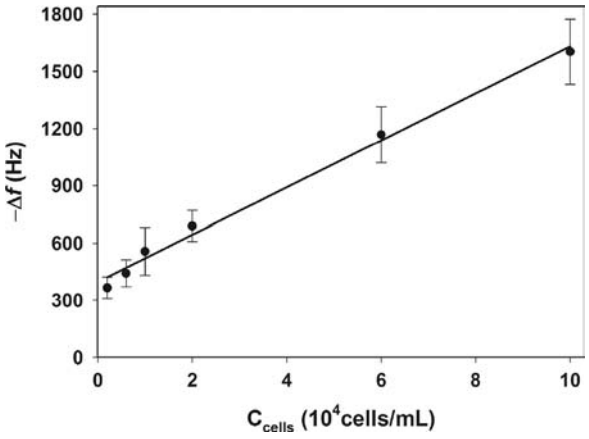

Fig. 6. The calibration curve of frequency response versus cell concentration. Each value is presented as mean ± S.D. ($n=3$).

Second, silver-enhanced AuNPs label method further enhances the sensitivity via the signal amplification of QCM response.

3.4. Fluorescence microscopic observation

In order to further confirm that the constructed sensor was specific to CCRF-CEM cells, we used acridine orange (AO) to stain the cells captured on different electrodes surfaces and observed with the fluorescence microscope under blue light irradiation. As shown in Fig. 7, no green dots could be observed on the AO-stained sgc8c electrode without incubation of cells (image A). The number of CCRF-CEM cells captured by the aptamer-modified electrode was the largest (image B), while CCRF-CEM cells on the random nucleotide-modified electrode surface could be negligible (image C). Another control experiment was conducted using Romas cells, another kind of leukemia cells, and it has been observed that there were only a few cells adhered on the aptamer-modified electrode (image D). These results were in line with the aforementioned results obtained by the QCM measurement, all suggesting the excellent selectivity of the sensor towards target cancer cells. Taking various kinds of aptamers for cells into account, the proposed method can be applied for the specific detection of CCRF-CEM cells and many other kinds of cancer cells if appropriate aptamers are selected.

4. Conclusions

A QCM biosensor was designed for the selective detection of leukemia cell based on APBA-AuNPs catalyzed silver enhancement. CCRF-CEM cells could be effectively captured on the sensor surface via the specific interaction with the aptamer, and the application of silver-enhanced AuNP label effectively amplified the signal within a short time, which allowed for the sensitive detection of

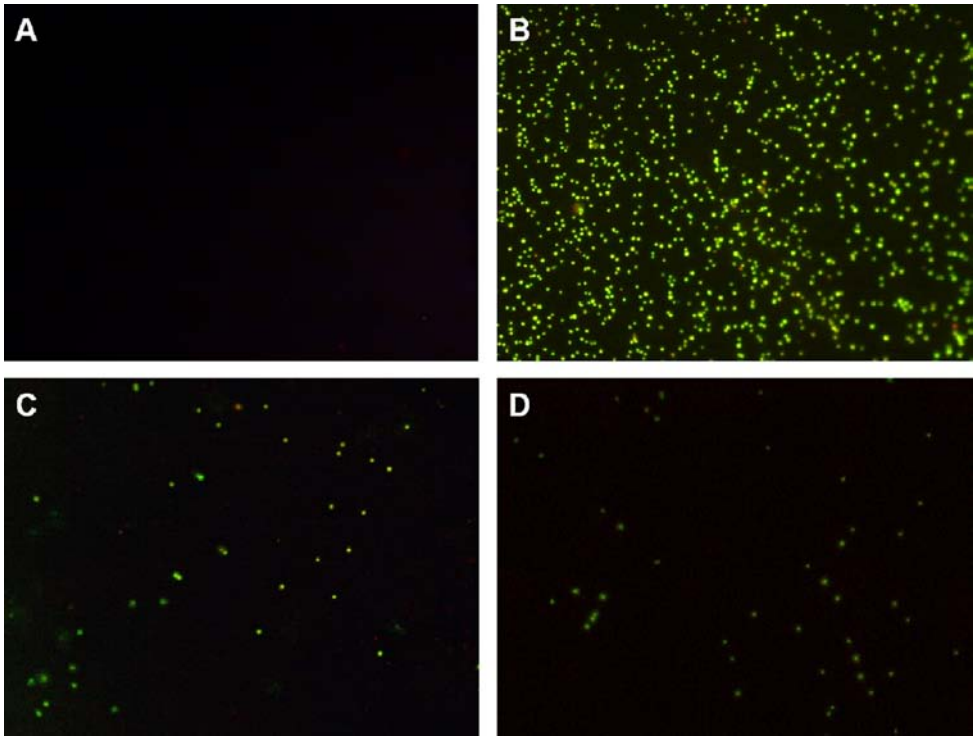

Fig. 7. Fluorescence microscopy images for different electrodes surfaces stained with acridine orange: (A) sgc8c electrode, (B) sgc8c electrode incubated with CCRF-CEM cells, (C) random nucleotide electrode incubated with CCRF-CEM cells, and (D) sgc8c electrode incubated with Romas cells. The electrodes were incubated with 10,000 cells for 30 min, and the images were recorded under blue light irradiation. (For interpretation of the references to color in this figure legend, the reader is referred to the web version of this article.)

the target cells. Furthermore, this method is simple, economical and fast for the analysis of cancer cells with satisfactory specificity, and this approach is of great potential for cancer cell detection.

Acknowledgment

This work was supported by the National Natural Science Foundation of China (Nos. 21235002, 21221003, 21222507 and 20975032).

References

[1] R. Siegel, D. Naishadham, A. Jemal, CA Cancer J. Clin. 62 (2012) 10–29.
[2] J.M. Peters, M.Q. Ansari, Arch. Pathol. Lab. Med. 135 (2011) 44–54.
[3] R.A. Ghossein, S. Bhattacharya, Eur. J. Cancer 36 (2000) 1681–1694.
[4] R. Misra, S.K. Sahoo, Mol. Pharm. 8 (2011) 852–866.
[5] A.D. Ellington, J.W. Szostak, Nature 346 (1990) 818–822.
[6] C. Tuerk, L. Gold, Science 249 (1990) 505–510.
[7] V. Bagalkot, O.C. Farokhzad, R. Langer, S. Jon, Angew. Chem. Int. Ed. 45 (2006) 8149–8152.
[8] A.N. Kawde, M.C. Rodriguez, T.M.H. Lee, J. Wang, Electrochem. Commun. 7 (2005) 537–540.
[9] H.P. Dwivedi, R.D. Smiley, L.A. Jaykus, Appl. Microbiol. Biotechnol. 97 (2013) 3677–3686.
[10] S.D. Jayasena, Clin. Chem. 45 (1999) 1628–1650.
[11] T. Deng, J. Li, L.L. Zhang, J.H. Jiang, J.N. Chen, G.L. Shen, R.Q. Yu, Biosens. Bioelectron. 25 (2010) 1587–1591.
[12] M. Zhang, H. Liu, L. Chen, M. Yan, L. Ge, S. Ge, J. Yu, Biosens. Bioelectron. 49 (2013) 79–85.
[13] D. Tan, Y. He, X. Xing, Y. Zhao, H. Tang, D. Pang, Talanta 113 (2013) 26–30.
[14] J.S. Lee, M.S. Han, C.A. Mirkin, Angew. Chem. 119 (2007) 4171–4174.
[15] Y. Zhang, Z. Tang, J. Wang, H. Wu, A. Maham, Y. Lin, Anal. Chem. 82 (2010) 6440–6446.
[16] H. Zhang, L. Wang, W. Jiang, Talanta 85 (2011) 725–729.
[17] J.M. Bergen, H.A. von Recum, T.T. Goodman, A.P. Massey, S.H. Pun, Macromol. Biosci. 6 (2006) 506–516.
[18] X. Huang, P.K. Jain, I.H. El-Sayed, M.A. El-Sayed, Nanomedicine 2 (2007) 681–693.
[19] J. Ai, Y. Xu, B. Lou, D. Li, E. Wang, Talanta 118 (2014) 54–60.
[20] S. Gupta, S. Huda, P.K. Kilpatrick, O.D. Velev, Anal. Chem. 79 (2007) 3810–3820.
[21] X. Jia, L. Tan, Q. Xie, Y. Zhang, S. Yao, Sens. Actuators B: Chem. 134 (2008) 273–280.
[22] C. Modin, A.L. Stranne, M. Foss, M. Duch, J. Justesen, J. Chevallier, L.K. Andersen, A.G. Hemmersam, F.S. Pedersen, F. Besenbacher, Biomaterials 27 (2006) 1346–1354.
[23] P.I. Reyes, Z. Duan, Y. Lu, D. Khavulya, N. Boustany, Biosens. Bioelectron. 41 (2013) 84–89.
[24] X.L. Wei, Z.H. Mo, B. Li, J.M. Wei, Colloids Surf. B: Biointerfaces 59 (2007) 100–104.
[25] J. Fatisson, F. Azari, N. Tufenkji, Biosens. Bioelectron. 26 (2011) 3207–3212.
[26] Z. Fohlerová, J. Turánek, P. Skládal, Sens. Actuators B: Chem. 174 (2012) 153–157.
[27] Y. Pan, M. Guo, Z. Nie, Y. Huang, C. Pan, K. Zeng, Y. Zhang, S. Yao, Biosens. Bioelectron. 25 (2010) 1609–1614.
[28] D. Shangguan, Z. Tang, P. Mallikaratchy, Z. Xiao, W. Tan, ChemBioChem 8 (2007) 603–606.
[29] Y. Pan, W. Shan, H. Fang, M. Guo, Z. Nie, Y. Huang, S. Yao, Biosens. Bioelectron. 52 (2014) 62–68.
[30] M. Guo, J. Chen, Y. Zhang, K. Chen, C. Pan, S. Yao, Biosens. Bioelectron. 23 (2008) 865–871.
[31] M.A. Ali, S. Srivastava, M.K. Pandey, V.V. Agrawal, R. John, B.D. Malhotra, Anal. Chem. 86 (2014) 1710–1718.
[32] B. Jeong, R. Akter, O.H. Han, C.K. Rhee, M.A. Rahman, Anal. Chem. 85 (2013) 1784–1791.
[33] D. Shangguan, Z. Cao, L. Meng, P. Mallikaratchy, K. Sefah, H. Wang, Y. Li, W. Tan, J. Proteome Res. 7 (2008) 2133–2139.
[34] A. Matsumoto, N. Sato, K. Kataoka, Y. Miyahara, J. Am. Chem. Soc. 131 (2009) 12022–12023.
[35] G. Sauerbrey, Z. Phys. 155 (1959) 206–222.
[36] H. He, Q. Xie, Y. Zhang, S. Yao, J. Biochem. Biophys. Methods 62 (2005) 191–205.
[37] X. Tu, Q. Xie, C. Xiang, Y. Zhang, S. Yao, J. Phys. Chem. B 109 (2005) 4053–4063.
[38] J.J. Zhang, M.M. Gu, T.T. Zheng, J.J. Zhu, Anal. Chem. 81 (2009) 6641–6648.
[39] H. Wang, H. Zeng, Z. Liu, Y. Yang, T. Deng, G. Shen, R. Yu, Anal. Chem. 76 (2004) 2203–2209.